ЖЭТФ, 2006, том 129, вып. 1, стр. 63–70

MODIFICATION OF THE Xe $4d$ GIANT RESONANCE BY THE C_{60} SHELL IN MOLECULAR Xe@C_{60}

M. Ya. Amusia [a,c], ***A. S. Baltenkov*** [b*], ***L. V. Chernysheva*** [c], ***Z. Felfli*** [d], ***A. Z. Msezane*** [d]

[a] *Racah Institute of Physics, The Hebrew University*
91904, Jerusalem, Israel

[b] *Arifov Institute of Electronics*
700125, Akademgorodok, Tashkent, Uzbekistan

[c] *Ioffe Physical-Technical Institute*
194021, St. Petersburg, Russia

[d] *Department of Physics and Center for Theoretical Studies of Physical Systems, Clark Atlanta University*
30314, Atlanta GA, USA

Submitted 28 June 2005

It is demonstrated that in photoabsorption of the $4d^{10}$ subshell of a Xe atom in molecular Xe@C_{60}, the $4d$ giant resonance that characterizes the isolated Xe atom is distorted significantly. The reflection of photoelectron waves by the C_{60} shell leads to profound oscillations in the photoionization cross section such that the Xe giant resonance is transformed into four strong peaks. Similarly, the angular anisotropy parameters, both dipole and nondipole, are also modified. The method of calculation is based on the approximation of the C_{60} shell by an infinitely thin bubble potential that leaves the sum rule for the $4d$-electrons almost unaffected, but noticeably modifies the dipole polarizability of the $4d$-shell.

PACS: 32.80.Fb, 32.80.Hd

1. INTRODUCTION

Giant resonances are universal features of the excitation of finite many-fermion systems: nuclei, atoms, fullerenes, and clusters. They represent collective, coherent oscillations of many particles and manifest themselves most prominently in photon absorption cross sections. In a nucleus, giant resonances represent the excitation of coherent oscillatory motion of all protons relative to all neutrons [1], while in all the other objects mentioned above, they represent the coherent motion of all electrons of at least one many-electron shell (in atoms) and all collective electrons in metallic clusters and fullerenes. Giant resonances are manifestations of plasmon-type or Langmuir excitations in a homogeneous electron gas [2] or the so-called «zero» sound in a Fermi liquid [3].

The universal nature of the giant resonances (GRs) was recently emphasized [4]. In photoabsorbtion cross sections, GRs are represented as a function of photon energy by huge, almost symmetric broad maxima. They have very large so-called oscillator strengths, which are determined by the total integrated area of the photoabsorption cross-section curves. The similarity of GRs in different objects is amazing, because when plotted on the same relative scales, GRs in nuclear Pb, $4d^{10}$ subshell in atomic Xe and in fullerene C_{60} look alike [4]. It is important to emphasize that the ratio of the resonance width Γ that characterizes its lifetime τ, $\tau \sim 1/\Gamma$, to the frequency Ω is almost the same for the above-mentioned objects,

$$1/5 \leq \Gamma/\Omega \leq 1/4.$$

It is obvious that the absolute values of the resonance energies and cross sections differ in these objects by orders of magnitude, particularly when we compare the values for the $4d^{10}$ subshell in atomic Xe and nuclear Pb.

At first glance, a GR represents an immanent, inner feature of an object. However, it is of interest to

*E-mail: arkbalt@mail.ru

understand whether at all and under what conditions GRs could be modified. From [2–4], it is clear that the frequency of GRs could be modified by altering the density of collective electrons in atoms and multiatomic objects or nucleons in nuclei. Needless to say, it is practically impossible to do. Hence, the direct verification of the theories developed in [2] and [3] concerning GRs is impossible. Collecting large numbers of Fermi atoms in a trap at low temperature can create a semi-natural object for studies of GRs' dependence on the density as well as of the universality of GRs. It is reasonable to expect such experiments in the not too distant future.

However, one can imagine another way of altering the GR's frequency, structure, and even their very existence. It seems that this can be achieved by placing objects possessing GRs into a cage that resonates. Indeed, the recently discovered endohedral atoms present the possibility of creating such an object: viz., an atom of Xe that has a GR in its $4d^{10}$ subshell placed inside a C_{60} shell, Xe@C_{60}. One can argue that in Xe@C_{60}, it is not the GR that is modified, but its observable manifestation. We believe, however, that the possibility to affect such a decisively important manifestation as the photoabsorption cross section is both of interest and of importance.

The photoionization of endohedral atoms, A@C_{60}, was studied in a number of papers [5–8]. The physical reason for the modification of the total cross sections and angular distributions, both dipole and nondipole, is in the reflection of the relatively slow photoelectron by the C_{60} shell. The effect of C_{60} rapidly disappears with the growth of the photoelectron energy. This is why giant autoionization resonances, e.g., those in Eu [9], remain unaffected by the C_{60} shell, because relatively fast photoelectrons are emitted after their excitation.

In this paper, we calculate the photoionization cross section and the angular anisotropy parameters of Xe@C_{60}, representing the C_{60} by a delta-type potential. The range of validity of this approximate potential is discussed at length in a recent paper [10]. Contrary to photon absorption, photon scattering is not accompanied by a strong reflection of the emitted object by the C_{60} shell. In order to see how the latter affects the photon scattering in the GR region, we calculate the dipole polarizability of Xe@C_{60} and also check the sum rule of the GR in Xe and Xe@C_{60}.

2. SOME DETAILS OF CALCULATIONS

The description of the interaction of electromagnetic radiation with fullerene-like molecules A@C_{60} is a very complicated theoretical problem, an order of magnitude more complex than the calculation for an isolated atom. Therefore, to analyze the influence of the fullerene shell encapsulating an endohedral atom, considerable simplifications are almost inevitable. These simplifications can be introduced because the geometrical size of a fullerene cage is significantly larger than the radius of any subshell of the encapsulated atom. Therefore, to a good approximation, the initial state wave function of an endohedral atom A@C_{60} is the same as the wave function of the isolated atom A. The surrounding carbon atoms of C_{60} need to be taken into account only to describe the final state of the photoionization process, the molecular continuum wave function.

Further, for a low-energy photoelectron with the wavelength $\lambda \sim 1/k$ (k being the photoelectron momentum in atomic units) of the order of or larger than the distance between the C atoms forming the fullerene cage, the real C_{60} potential can be approximated quite well by the potential of a spherical shell formed by the smeared-on-the-sphere carbon atoms. Even for higher energy (momentum) photoelectrons, the spherical shell potential is not a bad approximation at all (see [10] and the references therein). In any case, for the description of the photoionization of the atom A in molecular A@C_{60}, the real potential of the fullerene cage is replaced by a spherically symmetric phenomenological potential $V(r)$ concentrated on the surface of the cage with parameters defined by the experimental data for an empty fullerene cage.

If the photoelectron wavelength is of the order of the bond length between the C atoms, it is clearly larger than the thickness of the spherical shell where $V(r) \neq 0$. We therefore approximate the spherical shell as the one of zero thickness. This allows the determination of the continuum wave function by matching the inner and outer solutions of the Schrödinger equation at the boundary. The situation here is similar to nuclear physics, where low-energy nucleon scattering can be described by a logarithmic derivative of the wave function at $r = 0$. This derivative, in turn, is defined by the nucleon binding energy [11]. In our case, the boundary condition for the photoelectron wave function is imposed not at zero but on the sphere of the radius R. This method of defining the wave function is equivalent to representing the shell potential as a bubble potential

$$V(r) = -V_0\delta(r - R).$$

Here, R is the fullerene radius known from experimental data and V_0 is the δ-potential effective strength,

determined by the electron affinity of an «empty» C_{60} molecule.

As in any simplification, the bubble potential has its limited domain of validity. But its application is reasonable for the description of the electronic processes involving C_{60} for which the details of the wave function inside the spherical layer (where the C atoms are concentrated) are insignificant. Among these processes are photo-detachment of the negative C_{60}^- ions [12], elastic scattering of slow electrons by fullerenes [13], confinement resonances in the photoionization of endohedral atoms A@C_{60} [10], etc. In this paper, we use the bubble potential to model the actual potential and describe the dipole $\beta(\omega)$ and nondipole $\gamma(\omega)$ parameters in the photoelectron angular distribution from endohedral atoms Xe@C_{60}.

The formulas used in this paper have been derived in Ref. [7], and we therefore present only the main results here. For an atom A located at the center of a C_{60} cage, the problem of calculating the wave function of an electron in the continuum is, in the one-electron approximation, reduced to solving the one-dimensional Schrödinger equation, in which the bubble potential is added to the potential of an isolated atom A. It is evident that the solutions of this equation inside and outside the sphere of radius R are the wave functions of the isolated atom A. Therefore, inside the potential bubble, the continuum wave function differs only by a normalization factor dependent on the photoelectron energy from the regular solution $u_{kl}(r)$ of the Schrödinger equation for a free atom, i.e.,

$$\chi_{kl}(r) = T_l(k) u_{kl}(r),$$

with l being the electron angular momentum. Outside the δ-sphere, the function $\chi_{kl}(r)$ is a linear combination of the regular $u_{kl}(r)$ and irregular $v_{kl}(r)$ solutions of this equation. The coefficients of the linear combination are defined by the matching conditions of the wave functions on the spherical shell, i.e., at $r = R$. The additional phase shift $\Delta_l(k)$ of the wave function due to electron scattering by the bubble potential and the coefficient $T_l(k)$ are defined by the matching conditions at $r = R$ as

$$\begin{aligned} \operatorname{tg}\Delta_l(k) &= \frac{u_{kl}^2(R)}{u_{kl}(R)v_{kl}(R) - k/\Delta L}, \\ T_l(k) &= \cos\Delta_l(k)\left[1 - \operatorname{tg}\Delta_l(k)\frac{v_{kl}(R)}{u_{kl}(R)}\right], \end{aligned} \qquad (1)$$

where ΔL is the discontinuity of the logarithmic derivative of the wave function at $r = R$, related to the fullerene radius R and the electron affinity I of the empty C_{60} via

$$\Delta L = -2V_0 = -\beta[1 + \operatorname{cth}(\beta R)],$$

where $\beta = \sqrt{2I}$. Throughout the text, the atomic system of units ($\hbar = m = e = 1$) is used. We note that in deriving Eq. (1), we take into account that the Wronskian of the radial Schrödinger equation is given by

$$W_{kl}(r) = u_{kl}(r)v'_{kl}(r) - u'_{kl}(r)v_{kl}(r) = k \neq 0.$$

As long as the «size» of the atomic subshell is smaller than the size of C_{60}, the matrix elements for electron transitions to the continuum are formed near atom A, i.e., well inside the C_{60}-sphere. Therefore, these amplitudes coincide with the amplitudes of the corresponding transitions in the free atom except for the multiplicative factor $T_l(k)$. Because of the coupling between the oscillations of the wave functions inside and outside this sphere, the coefficients have a resonance character. Therefore, there are resonances in the transition matrix elements for endohedral atoms that translate into the so-called confinement resonances in the total photoionization cross section [7, 10, 14], which in the case of Xe@C_{60} are superimposed on the $4d^{10}$ Xe giant resonance. It is evident that for the same reason, these new resonances also appear in the dipole and nondipole asymmetry parameters.

The expressions for these parameters can be simply obtained from the general expressions for the dipole and nondipole asymmetry parameters derived for free atoms [15–17], where it is only necessary to replace the dipole $d_{l\pm1}$ and quadrupole $q_{l\pm2,0}$ matrix elements by $T_{l\pm1}d_{l\pm1}$ and $T_{l\pm2,0}q_{l\pm2,0}$ respectively, and the corresponding phase shifts of the photoelectron wave functions for the free atom $\delta_{l\pm1}$ and $\delta_{l\pm2,0}$ by the sum of the phases:

$$\delta_{l\pm1} + \Delta_{l\pm1} \quad \text{and} \quad \delta_{l\pm2,0} + \Delta_{l\pm2,0}.$$

We focus on the dipole parameter $\beta_{nl}(\omega)$ defining the angular distribution in photoionization of the atomic d-subshells and on the nondipole parameters $\gamma_{nl}^C(\omega)$ and $\delta_{nl}^C(\omega)$. The angular distribution for isolated atoms is given by the expression [15]

$$\begin{aligned} \frac{d\sigma_{nl}(\omega)}{d\Omega} = \frac{\sigma_{nl}(\omega)}{4\pi}&[1 + \beta_{nl}(\omega)P_2(\cos\theta) + \\ &+ [\delta_{nl}^C(\omega) + \gamma_{nl}^C(\omega)\cos^2\theta]\sin\theta\cos\phi], \end{aligned} \qquad (2)$$

where $\sigma_{nl}(\omega)$ is the total photoionization cross section, $\beta_{nl}(\omega)$ is the dipole angular anisotropy parameter,

$\gamma^C_{nl}(\omega)$ and $\delta^C_{nl}(\omega)$ are the nondipole asymmetry parameters, $P_2(\cos\theta)$ is the Legendre polynomial, θ is the polar angle of the photoelectron velocity with respect to the photon polarization vector $\mathbf{e}$, and ϕ is the azimuthal angle defined by the projection of the electron velocity in the plane perpendicular to $\mathbf{e}$ and containing the photon propagation vector $\boldsymbol{\kappa}$.

The dipole parameter $\beta_{4d}(\omega)$ is given by

$$\beta_{4d} = \frac{2}{5(2d_1^2+3d_3^2)}\Big[d_1^2+6d_3^2-18d_1d_3\cos(\delta_3-\delta_1)\Big]. \quad (3)$$

The nondipole asymmetry parameters $\gamma^C_{nl}(\omega)$ and $\delta^C_{nl}(\omega)$ are related to $\gamma_{nl}(\omega)$ and $\eta_{nl}(\omega)$ introduced in [18] and expressed there via the dipole d and quadrupole q matrix elements. Here, we are interested in the case where $n = 4$, $l = 2$. Therefore, we have

$$\begin{aligned}\delta^C_{4d} &= \frac{\omega}{c}\Big(\gamma_{4d}+\eta_{4d}\Big),\\ \gamma^C_{4d} &= -5\frac{\omega}{c}\eta_{4d},\end{aligned} \quad (4)$$

where c is the speed of light. The coefficients $\gamma_{4d}(\omega)$ and $\eta_{4d}(\omega)$ are given by

$$\begin{aligned}\gamma_{4d} = &-\frac{6}{35(2d_1^2+3d_3^2)}\times\\ &\times\Big[7d_1[q_0\cos(\delta_0-\delta_1)-q_2\cos(\delta_2-\delta_1)]+\\ &+3d_3[q_2\cos(\delta_2-\delta_3)-6q_4\cos(\delta_4-\delta_3)]\Big], \quad (5)\end{aligned}$$

$$\begin{aligned}\eta_{4d} = &-\frac{6}{35(2d_1^2+3d_3^2)}\times\\ &\times\Big[2d_1[q_2\cos(\delta_2-\delta_1)-6q_4\cos(\delta_4-\delta_1)]+\\ &+d_3[7q_0\cos(\delta_0-\delta_3)-8q_2\cos(\delta_2-\delta_3)+\\ &+6q_4\cos(\delta_4-\delta_3)]\Big]. \quad (6)\end{aligned}$$

In these formulas, $d_{1,3}$ and $q_{0,2,4}$ are the dipole and quadrupole matrix elements in the one-electron Hartree–Fock approximation and $\delta_i(\epsilon)$ are the photoelectron's elastic scattering phase shifts, $\epsilon = \omega - I_{4d}$, with I_{4d} being the $4d$-subshell ionization potential. The matrix elements are defined as

$$\begin{aligned}d_{1,3} \equiv d_{4d,k1,3} &= \int_0^\infty u_{4d}(r)ru_{k1,3}(r)\,dr,\\ q_{0,2,4} \equiv q_{4d,k0,2,4} &= \frac{1}{2}\int_0^\infty u_{4d}(r)r^2u_{k0,2,4}(r)\,dr,\end{aligned} \quad (7)$$

where $u_{4d}(r)$ and $u_{kl}(r)$ are the radial parts of the Hartree–Fock one-electron wave functions. To obtain the corresponding expressions for the parameters in Eqs. (3), (5), and (6), we must perform the following substitutions in them [16, 18]:

$$|d_{1,3}|^2 \to D'^2_{1,3}+D''^2_{1,3},$$

$$\begin{aligned}d_iq_j\cos(\delta_j-\delta_i) \to &\Big(D'_iQ'_j+D''_iQ''_j\Big)\cos(\delta_j-\delta_i)-\\ &-\Big(D'_iQ''_j-D''_iQ'j\Big)\sin(\delta_j-\delta_i). \quad (8)\end{aligned}$$

Here, $D'_{1,3}$, $Q'_{0,2,4}$ and $D''_{1,3}$, $Q''_{0,2,4}$ are respectively the real and imaginary parts of the corresponding matrix elements. The presence of the bubble potential modifies Eqs. (3), (5), and (6) to the respective equations

$$\begin{aligned}\beta_{4d} = &\frac{2}{5(2T_1^2d_1^2+3T_3^2d_3^2)}\Big[T_1^2d_1^2+6T_3^2d_3^2-\\ &-18T_1T_3d_1d_3\cos(\delta_3+\Delta_3-\delta_1-\Delta_1)\Big], \quad (9)\end{aligned}$$

$$\begin{aligned}\gamma_{4d} = &-\frac{6}{35(2T_1^2d_1^2+3T_3^2d_3^2)}\times\\ &\times\Big[7T_1d_1\ [T_0q_0\cos(\delta_0+\Delta_0-\delta_1-\Delta_1)-\\ &-T_2q_2\cos(\delta_2+\Delta_2-\delta_1-\Delta_1)]+\\ &+3T_3d_3[T_2q_2\cos(\delta_2+\Delta_2-\delta_3-\Delta_3)-\\ &-6T_4q_4\cos(\delta_4+\Delta_4-\delta_3-\Delta_3)]\Big], \quad (10)\end{aligned}$$

$$\begin{aligned}\eta_{4d} = &-\frac{6}{35(2T_1^2d_1^2+3T_3^2d_3^2)}\times\\ &\times\Big[2T_1d_1\ [T_2q_2\cos(\delta_2+\Delta_2-\delta_1-\Delta_1)-\\ &-6T_4q_4\cos(\delta_4+\Delta_4-\delta_1-\Delta_1)]+\\ &+T_3d_3[7T_0q_0\cos(\delta_0+\Delta_0-\delta_3-\Delta_3)-\\ &-8T_2q_2\cos(\delta_2+\Delta_2-\delta_3-\Delta_3)]+\\ &+6T_4q_4\cos(\delta_4+\Delta_4-\delta_3-\Delta_3)]\Big]. \quad (11)\end{aligned}$$

Because the photoelectron angular distributions parameters involve interference among amplitudes of different angular momenta, rather than just the sum of absolute squares that determines the total photoionization cross section, one can expect more complicated resonance structures in the energy dependence of these parameters and, hence, in the photoelectron angular

distributions than in the total photoionization cross sections.

We use the general formulas in Eqs. (1)–(11) to investigate the photoionization of the Xe@C_{60} molecule, with the Xe atom located at the center of the bubble potential. The wave functions of the free Xe atom in the $4d$-state and in the continuum $u_{kl}(r)$ were calculated in the one-electron Hartree–Fock approximation using the computer codes ATOM [19]. The solutions $v_{kl}(r)$ irregular at $r = 0$ were calculated, as in Ref. [7, 10], using the relation

$$v_{kl}(r) = u_{kl}(r)W_{kl}(r) \int \frac{dr}{u_{kl}^2(r)}. \qquad (12)$$

3. RESULTS OF CALCULATIONS

The calculated cross sections, dipole and nondipole parameters for the photoionization, and dipole polarizability of the Xe atom encapsulated in a C_{60} shell, Xe@C_{60}, are presented in Figs. 1–4. The corresponding parameters for the free Xe atom are also given there. Clearly, the fullerene shell qualitatively alters the dependence of these parameters on the photoelectron energy. Very impressive is its effect on the cross section, where the giant resonance in the isolated atom is transformed into four well-pronounced maxima in Xe@C_{60}, which is depicted in Fig. 1. The fifth maximum is very small. As in the case of the $4d - \epsilon f$ giant resonance in Ba atoms [20], the processes of reflection and refraction of p- and f-electronic waves by the fullerene shell in Xe@C_{60} also induce a resonance structure, and the total photoionization cross section $\sigma_{4d}(\omega)$, as a function of the photon energy, oscillates around the atomic «background».

Figure 2 presents the result for the dipole parameter $\beta_{4d}(\omega)$. Here, we again see very significant modifications by the action of the C_{60} shell; in fact, four maxima are observed instead of the two in pure Xe, including a very narrow one that appears just near the threshold. The curve for $\beta_{4d}(\omega)$ is modified stronger than that for the cross section, because it includes a product of d_1 and d_3 matrix elements along with a sum of their moduli squared. Figure 3 depicts data for both nondipole parameters $\gamma_{4d}^C(\omega)$ (Fig. 3a) and $\delta_{4d}^C(\omega)$ (Fig. 3b), and the usually measurable combination $\gamma_{4d}^C(\omega) + 3\delta_{4d}^C(\omega)$ (Fig. 3c). Clearly, the C_{60} shell modifies all these parameters. Particularly notable is the near-threshold modification of $\gamma_{4d}^C(\omega)$ resulting in a high maximum instead of a minimum. The rest of the curve is modified similarly to that of $\beta_{4d}(\omega)$. The $\delta_{4d}^C(\omega)$ curve acquires a multi-maximum structure due

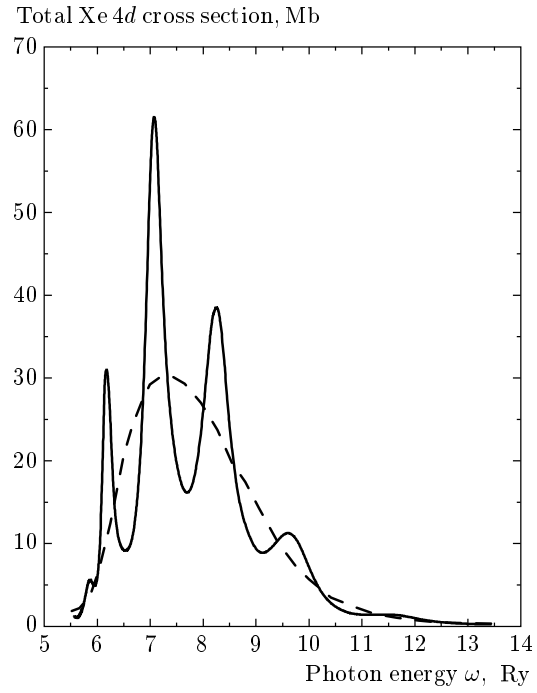

Fig. 1. Photoionization cross sections $\sigma_{4d}(\omega)$ of $4d$-electrons in atomic Xe (dashed curve) and in Xe@C_{60} (solid curve) as functions of the photon energy ω

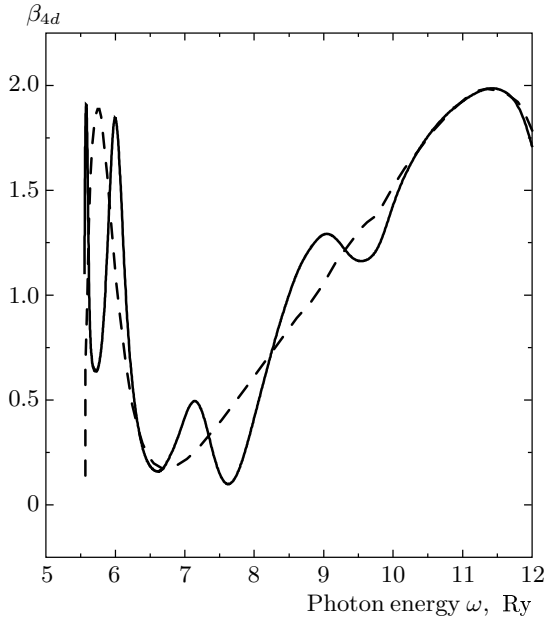

Fig. 2. Dipole angular anisotropy parameters $\beta_{4d}(\omega)$ of $4d$-electrons in atomic Xe (dashed curve) and in Xe@C_{60} (solid curve) as functions of the photon energy ω

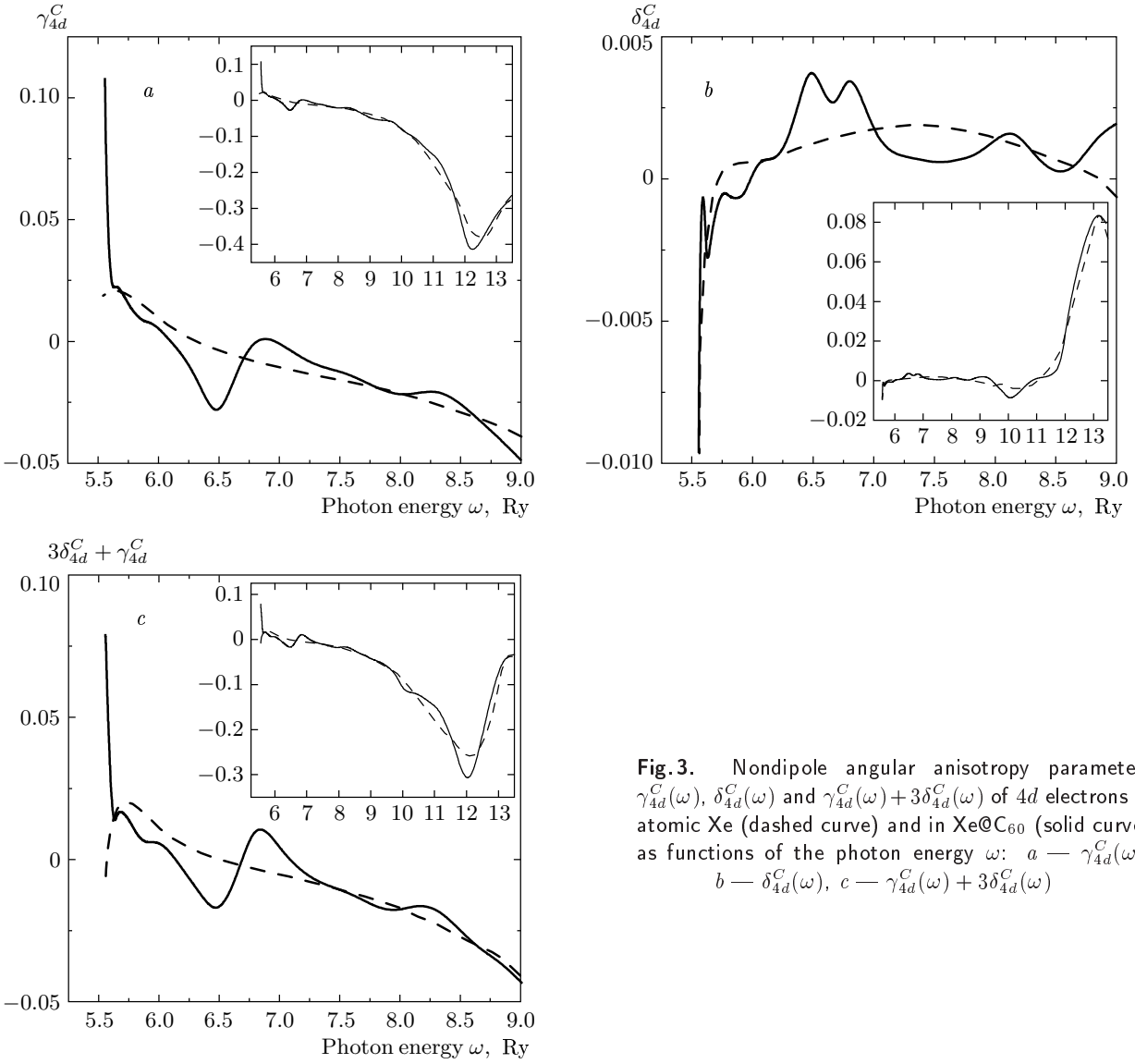

Fig. 3. Nondipole angular anisotropy parameters $\gamma^C_{4d}(\omega)$, $\delta^C_{4d}(\omega)$ and $\gamma^C_{4d}(\omega)+3\delta^C_{4d}(\omega)$ of $4d$ electrons in atomic Xe (dashed curve) and in Xe@C_{60} (solid curve) as functions of the photon energy ω: a — $\gamma^C_{4d}(\omega)$, b — $\delta^C_{4d}(\omega)$, c — $\gamma^C_{4d}(\omega) + 3\delta^C_{4d}(\omega)$

to the combination of dipole and quadrupole matrix elements that are modified differently by the C_{60} shell.

To clarify the effect of the C_{60} shell on the giant resonance, it is informative to compare dipole polarizabilities $\alpha_d^{(4d)}(\omega)$ for Xe and Xe@C_{60} in the giant resonance region 5.56Ry $\leq \omega \leq$ 13.45 Ry. Using the formula

$$\sigma_{4d}(\omega) = 4\pi\frac{\omega}{c}\,\mathrm{Im}\,\alpha_d^{(4d)}(\omega) \qquad (13)$$

we calculate the imaginary part of the polarizability. To find the real part of $\alpha_d^{(4d)}(\omega)$, the dispersion relation

$$\mathrm{Re}\,\alpha_d^{(4d)}(\omega) \approx \frac{2}{\pi}\int\limits_{I_{4d}}^{\infty}\frac{\omega'\,\mathrm{Im}\,\alpha_d^{(4d)}(\omega')}{\omega'^{\,2}-\omega^2}d\omega' = \frac{c}{2\pi^2}\int\limits_{I_{4d}}^{\infty}\frac{\sigma_{4d}(\omega')}{\omega'^{\,2}-\omega^2}d\omega' \qquad (14)$$

has to be used. In Eq. (14), we have neglected the contribution of discrete levels because their oscillator strengths are small for $4d$-electrons of either pure Xe or Xe@C_{60}. Figures 4*a*, *b* present the results for the polarizability of both Xe and Xe@C_{60}. The values of $\mathrm{Re}\,\alpha_d^{(4d)}(\omega)$ and $\mathrm{Im}\,\alpha_d^{(4d)}(\omega)$ are given in Fig. 4*a* and

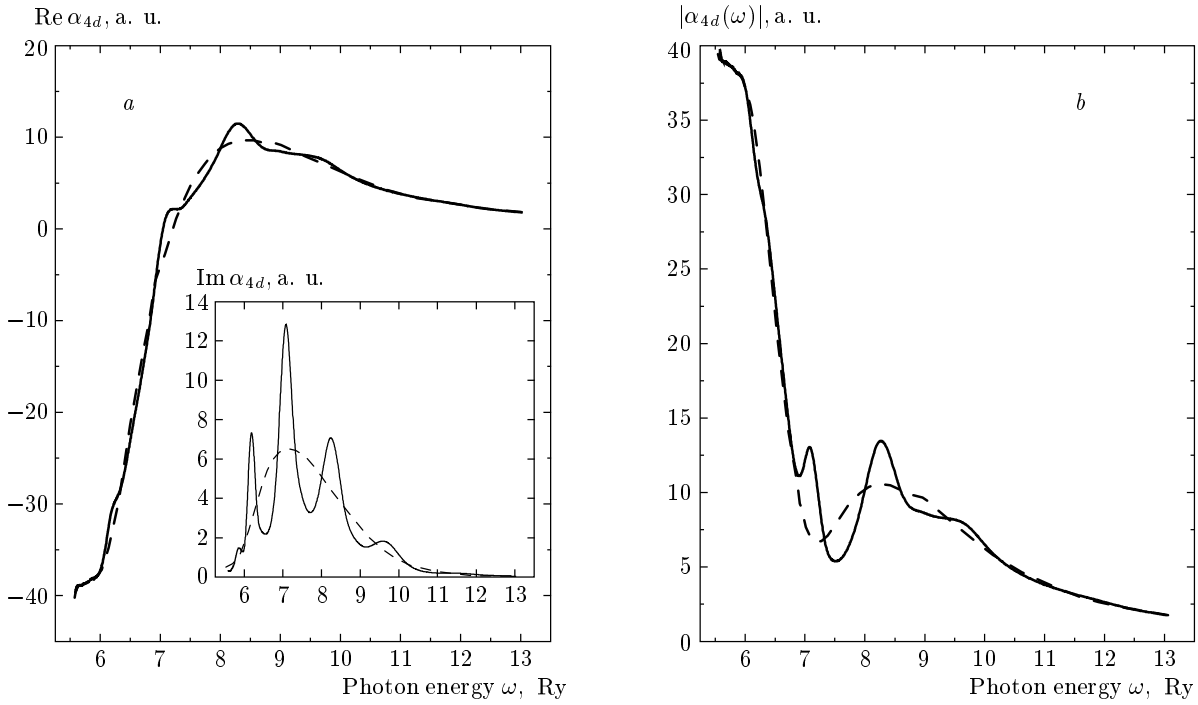

Fig. 4. Dipole polarizabilities $\alpha^C_{4d}(\omega)$ of $4d$-electrons in atomic Xe (dashed curve) and in Xe@C_{60} (solid curve) as functions of the photon energy ω. a — Real and imaginary parts of $\alpha^C_{4d}(\omega)$, b — absolute value of the polarizability $\alpha^C_{4d}(\omega)$

the rather informative $|\alpha_d^{(4d)}(\omega)|$ is depicted in Fig. 4*b*. We note that although the absolute value of $\alpha_d^{(4d)}(\omega)$ for Xe@C_{60} in the frequency region of interest is determined to a large extent by the sixty carbon atoms instead of a single Xe, they provide only a slowly decreasing contribution with increasing ω. The rapid variation of the polarizabilities must come from the Xe atom. Therefore, the results of our calculation for the polarizability can in principle be verified experimentally.

Physically, the origin of the new resonances is easy to understand. The photoelectron can escape from the atom directly, or scatter from the C_{60} shell on its way out. When the waves representing these two «pathways» are in phase, constructive interference, a resonant enhancement, results. When they are out of phase, destructive interference occurs. The decrease in the resonance structure with increasing photoelectron energy arises because, with increasing the energy, the C_{60} sphere becomes more and more transparent to the photoelectron, thereby decreasing the reflection and, thus, interference. In the general sense, the physical origin of these confinement resonances is the same as the cause of EXAFS in the photoabsorption of condensed matter, and the similar phenomenon in diatomic (and other) molecules.

It is interesting to note that while the cross section is strongly modified, the area under the curves for Xe and Xe@C_{60} within the giant resonance frequency region 5.56 Ry $\le \omega \le$ 13.45 Ry are almost the same. Indeed, the contribution of the $4d$-electrons to the sum rule

$$S_{4d} = \frac{c}{2\pi^2} \int\limits_{I_{4d}}^{\infty} \sigma_{4d}(\omega)\, d\omega$$

is equal to 10.61 and 10.53 for free Xe and Xe@C_{60}, respectively. These values are remarkably close to each other, emphasizing that the C_{60} shell causes redistribution of the $4d$ cross section leaving its total power unaltered. The calculated values are very close to the total number of electrons in the $4d$-shell, as expected. We note that with the increase of ω,

$$\mathrm{Re}\,\alpha_d \to -S_{4d}/\omega^2 \quad \text{as} \quad \omega \to \infty.$$

We checked this relation and found that the asymptotic value is reached relatively slowly. The Table illustrates this.

Finally, we note that the dramatic modification of the cross section and the dipole and nondipole angular anisotropy parameters, presented herein for Xe in Xe@C_{60}, will not be observed in the other endohedral

Asymptotic behavior of the real part of the polarizabilities for Xe and Xe@C_{60}

k	$\omega = I + k^2$, Ry	$\omega^2 \operatorname{Re}\alpha_{\mathrm{Xe}}$	$\omega^2 \operatorname{Re}\alpha_{\mathrm{Xe@C_{60}}}$
10	−105	−11.83	−11.74
20	−405	−10.90	−10.83
30	−905	−10.74	−10.66
50	−2505	−10.65	−10.58
150	−22505	−10.61	−10.54

atom Eu@C_{60}. The reason is that for the latter, the $4d^{10}$ giant resonance decays by emission of the outer subshell, i.e., relatively fast electrons that are not affected by the C_{60} shell.

4. CONCLUSION

According to the above calculation, the existence of the C_{60} shell in molecular Xe@C_{60} leads to strong distortions of both the total photoionization cross section and the dipole and nondipole asymmetry parameters within the $4d$ giant resonance regime. This is a vivid manifestation of the resonance nature of the C_{60} cage that acts as a resonator surrounding the ionized atom. We strongly urge the initiation of experimental investigations of this new effect to establish its existence, which could have important implications for the interpretation of molecular and condensed-matter photoelectron studies. Particularly interesting and relevant is the possibility of preparing a series of C_{60} fullerenes encapsulating either atoms or small molecules using the recent novel molecular surgery method [21] and performing photoabsorption measurements.

This work was supported by Binational Science Foundation (grant № 2002064), Israeli Science Foundation (grant № 174/03), USDoE, Division of Chemical Sciences, Office of Basic Energy Sciences, Office of Energy Research, AFOSR, the Hebrew University Intramural Fund and Uzbek Foundation (Award Ф-2-1-12).

REFERENCES

1. A. B. Migdal, *Theory of Finite Fermi Systems and Applications to Atomic Nuclei*, Wiley, Interscience, New York (1967).
2. D. Pines, *Elementary Excitations in Solids*, Benjamin, New York (1963).
3. L. D. Landau, Z. Exp. Teor. Fiz. **35**, 97 (1958).
4. M. Ya. Amusia and J.-P. Connerade, Rep. Prog. Phys. **63**, 41 (2000).
5. O. Frank and J.-M. Rost, Chem. Phys. Lett. **271**, 367 (1997).
6. M. Venuti, M. Stener, G. De Ati, and P. Decleva, J. Chem. Phys. **111**, 4589 (1999).
7. A. S. Baltenkov, Phys. Lett. A **254**, 203 (1999).
8. J.-P. Connerade, V. K. Dolmatov, P. A. Lakshmi, and S. T. Manson, J. Phys. B **32**, L239 (1999).
9. M. Ya. Amusia, L. V. Chernysheva, and S. I. Sheftel, J. Tech. Phys., Short Commun. (USSR Acad. Sci.) **51**, 2411 (1981).
10. M. Ya. Amusia, A. S. Baltenkov, V. K. Dolmatov, S. T. Manson and A. Z. Msezane, Phys. Rev. A **70**, 023201 (2004).
11. H. A. Bethe and P. Morrison, *Elementary Nuclear Theory*, Wiley, New York; Chapman & Hall, London (1956).
12. M. Ya. Amusia, A. S. Baltenkov, and B. G. Krakov, Phys. Lett. A **243**, 99 (1998).
13. L. L. Lohr and S. M. Blinder, Chem. Phys. Lett. **198**, 100 (1992).
14. M. Ya. Amusia, A. S. Baltenkov, and U. Becker, Phys. Rev. A **62**, 012701 (2000).
15. J. W. Cooper, Phys. Rev. A **47**, 1841 (1993).
16. M. Ya. Amusia, A. S. Baltenkov, L. V. Chernysheva, Z. Felfli, and A. Z. Msezane, Phys. Rev. A **63**, 052506 (2001) (and references therein).
17. M. Ya. Amusia, A. S. Baltenkov, L. V. Chernysheva, Z. Felfli, S. T. Manson, and A. Z. Msezane, Phys. Rev. A **67**, 60702 (2003).
18. M. Ya. Amusia, P. U. Arifov, A. S. Baltenkov, A. A. Grinberg, and S. G. Shapiro, Phys. Lett. A **47**, 66 (1974).
19. M. Ya. Amusia, L. V. Chernysheva, *Computation of Atomic Processes*, IOP Publishing Ltd, Bristol, Philadelphia (1997).
20. J. Luberek and G. Wendin, Chem. Phys. Lett. **248**, 147 (1996).
21. K. Komatsu, M. Murata, and Y. Murata, Science **307**, 238 (2005).